Structure of Pressure-Assisted Cold Denatured Lysozyme and Comparison with Lysozyme Folding Intermediates†

David P. Nash‡ and Jiri Jonas*,‡,§

Department of Chemistry, School of Chemical Sciences, University of Illinois at Urbana-Champaign, Urbana, Illinois 61801, and Beckman Institute for Advanced Science and Technology, University of Illinois at Urbana-Champaign, Urbana, Illinois 61801

Received April 15, 1997; Revised Manuscript Received September 16, 1997⊗

ABSTRACT: At high (>3.5 kbar) pressures and low (<−10 °C) temperatures, hen egg-white lysozyme denatures readily and reversibly. Amide hydrogen exchange methods were used to investigate the structure of the pressure-assisted cold-denatured state of lysozyme. Protection factors were obtained for 52 backbone amide protons. The extent of protection of many of these protons is markedly different from that in lysozyme denatured by high temperature, high urea concentration, or chemical modification; specifically, the protection factors are higher and are strongly correlated with elements of secondary structure present in the native state. Furthermore, the pattern of protection factors is similar to that observed in lysozyme during refolding from highly denatured states, particularly during the early stages (<3.5 ms) of refolding [Gladwin, S. T., & Evans, P. A. (1996) *Folding Des. 1*, 407]. Previous data on cold-denatured ribonuclease A were reevaluated and compared to known folding intermediates [Houry, W. A., & Scheraga, H. A. (1996) *Biochemistry 35*, 11734; Udgaonkar, J. B., & Baldwin, R. L. (1990) *Proc. Natl. Acad. Sci. U.S.A. 87*, 8197] to further test the supposition that the pressure-assisted cold-denatured states of proteins resemble the early folding stages.

Studying the denatured states of proteins has long been a major research interest for investigators interested in the folding and dynamics of proteins (Dyson & Wright, 1996). Although denaturation is a general process, different methods (e.g., thermal or chemical) cause denaturation in appreciably different ways on the molecular level; sometimes the final denatured states differ appreciably as well (Dill & Shortle, 1991). Differences in denatured states—small differences in residual structure, for example—affect how the protein begins to fold and how folding progresses. As a result, a detailed understanding of denatured states and the process of denaturation is important in protein folding studies (Dyson & Wright, 1996; Kim & Baldwin, 1990; Creighton, 1993; Buck et al., 1994). Our research group has been interested in denaturation methods obtainable with high pressure (Jonas & Jonas, 1994), particularly cold denaturation. Cold denaturation of proteins has been well demonstrated recently (Privalov, 1990; Zhang et al., 1995; Ballew et al., 1996). Unfortunately, detailed studies of the cold-denatured state have been difficult, since the temperatures required to denature proteins are usually below the freezing point of water. As a result, various techniques have been used, either to destabilize the protein and thus allow cold denaturation to be studied at higher temperatures, or to prevent solvent freezing. Here, as in previous cold denaturation research done in this laboratory (Zhang et al., 1995; Nash et al., 1996), we have used high pressure to depress the freezing point of water. By applying moderate hydrostatic pressure (2−4 kbar), which frequently does not denature stable proteins by itself, aqueous samples remain liquid at temperatures as low as −20 °C.

Many types of protein denaturation, especially thermal and chemical denaturation, leave little or no residual structure in many proteins. By contrast, previous work (Zhang et al., 1995; Nash et al., 1996) on pressure and cold denaturation has suggested that these methods can leave appreciable residual structure in proteins. In RNase A, for example (Zhang et al. 1995), the extent of residual structure, as measured by hydrogen exchange methods, is similar to that present in molten globules (Buck et al. 1994) and other well-characterized, partially structured proteins. By itself, such a result is interesting enough, but it becomes more important when related to modern protein folding studies. Structures that persist in a protein upon denaturation, even relatively mild denaturation, are likely to be highly stable. If no appreciable barriers exist to the *rapid* formation of such structures—e.g., if they are fairly small—they should be among the first to appear in the refolding of a protein.

If such a parallel can be drawn, various mildly denatured states would serve as useful models for species present early in refolding, with the advantage that such species could be studied for hours or even days, rather than fractions of a second. There is already considerable evidence that the equilibrium molten globules of some proteins, obtained under mildly denaturing conditions, are structurally similar to the early, collapsed states occurring when the protein begins to fold (Fink, 1995; Ptitsyn, 1995). Since the pressure and cold-denatured states of RNase A appear to be similar to a

† This work was supported by National Institutes of Health Grant No. PHS 5 RO1 GM 42452.

* Author to whom correspondence should be addressed.

‡ Department of Chemistry.

§ Beckman Institute.

⊗ Abstract published in *Advance ACS Abstracts,* November 1, 1997.

[1] Abbreviations: Lysozyme, hen egg-white lysozyme; RNase A, bovine pancreatic ribonuclease A; TSP, sodium salt of 3-(trimethylsilyl)-propionic-2,2,3,3-d_4 acid (chemical shift reference); pH*, uncorrected pH meter reading in D_2O solutions; pH_{min}, pH of minimum exchange rate for amide protons in polypeptides.

S0006-2960(97)00881-7 CCC: $14.00

collapsed unfolded state, at least in terms of amide hydrogen protection (Nash et al. 1996) and absence of large-scale structure, cold and pressure denaturation may constitute a similarly mild form of denaturation, one possibly applicable to proteins that do not readily form equilibrium molten globules. Hence, a major motivation for this research is to characterize more proteins by cold denaturation and compare them to known species observed during folding.

Lysozyme was chosen, in this study, for several reasons. Lysozyme is a small, well-characterized protein that has been extensively studied before. The solution NMR structure is known (Redfield & Dobson, 1988; Miranker et al. 1991). Numerous studies have been made on the structure of lysozyme in denatured states (Buck et al. 1994) and during folding (Radford et al. 1992; Gladwin & Evans, 1996). A detailed study of the cold-denatured state, however, is lacking. The cold-denatured state of RNase A has been characterized before (Nash et al. 1996), and structure present in this state has been described. A comparison of several proteins is important to establish whether any parallels observed between the cold-denatured state and folding intermediates (Houry & Scheraga, 1996; Udgaonkar & Baldwin, 1990) are general, or whether they are specific to a given protein.

MATERIALS AND METHODS

Materials: Hen egg-white lysozyme (Sigma, catalog no. L-6876) was used without further purification. Solutions for the hydrogen exchange study consisted of 4 mM lysozyme, 20 mM d_2-maleic acid prepared directly from the anhydride, and 1.5 mM TSP in D_2O. Maleic acid was chosen as a buffer since its ionization has a low reaction volume and hence its pH is nearly pressure-independent (Kitamura & Itoh, 1987) over a wide pressure range. The pH* of the solutions was adjusted to 2.00 with dilute (8% in D_2O) DCl. A pH* of 2.0 destabilizes lysozyme sufficiently to make its cold denaturation observable with the help of pressure, but does not cause drastic structural changes under ambient conditions.

Pressure and Temperature Optimization. Conditions for cold denaturation were optimized by 1D proton NMR spectra, obtained with high-pressure NMR apparatus in our laboratory. The pressure vessels, pressure-generating apparatus, and high-pressure NMR probes have been described previously (Jonas et al. 1993). Spectra of lysozyme solutions of the same concentration and pH* used for the kinetic studies were obtained over a range of temperatures and pressures, using a 300 MHz GN-300 spectrometer equipped with a Tecmag Scorpio pulse programmer and MacNMR 5.4 software for spectrum acquisition and processing. The extent of denaturation was monitored by observing the sharp resonance of the ϵ_1 ring proton in histidine 15, which is well separated from other resonances (Samarasinghe et al. 1992) and shows a marked chemical shift change upon denaturation. Cold denaturation of lysozyme was found to be nearly complete at pressures above 3500 bar and temperatures below −12 °C (Figure 1). The conditions for all cold denaturation kinetic experiments in this study were 3725 ± 25 bar and −13.0 ± 0.6 °C, conditions that assure near complete cold denaturation while still avoiding freezing.

At the temperatures used for cold denaturation, the unfolding rate of lysozyme is sufficiently slow (∼1/h) that care must be taken to ensure denaturation is complete.

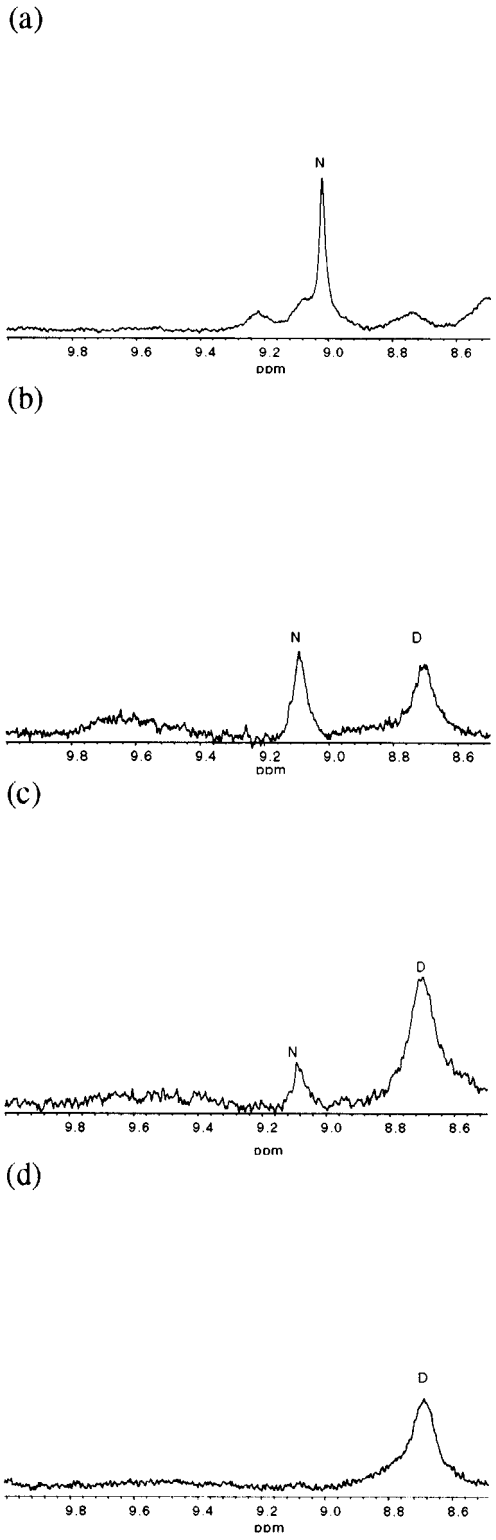

FIGURE 1: 1D proton NMR spectra of lysozyme under various conditions, showing the peak of the ϵ_1 ring proton in H15 in the native (N) and denatured (D) states. (a) $P = 1$ bar, $T = +11.8$ °C. (b) $P = 3500$ bar, $T = -10.4$ °C. (c) $P = 3500$ bar, $T = -15.2$ °C; incomplete equilibration (27 min) to denatured state. (d) $P = 3720$ bar, $T = -12.9$ °C; after overnight (8.5 h) equilibration. Hydrogen exchange experiments were performed under the conditions of figure 1d.

Figure 1, parts c and d, illustrates the effect of incomplete equilibration: the spectrum taken in 1c, under conditions similar to those used for the hydrogen exchange measurements, shows a small amount of residual native state (∼10%). The residual folded protein is a consequence of taking the

Table 1: Equilibration to Cold-Denatured State after Rapid Application of Cold-Denaturing Conditions (P = 3725 bar, T = +25.5 °C to P = 3725 bar, T = −13.2 °C)

time (min)	% native	ln (% native)
27	28.0	3.332
33	21.0	3.045
44	13.5	2.603
52	8.3	2.116

spectrum too soon (27 min after the final temperature was reached). Table 1 shows the progress of equilibration toward near-complete denaturation as a function of time at $P = 3725$ bar and $T = -13.2$ °C, conditions nearly identical to those used for hydrogen exchange. From the data in Table 1, a time of more than 1 h is needed for full equilibration and an accurate assessment of the amount of native state actually present. Figure 1d shows the absence of native state when equilibration is complete (8.5 h under cold denaturing conditions).

Assuming a two-state denaturation process, the equilibration reaction is first order and hence ln (%N) vs time is linear. The results of least-squares fitting the data in Table 1 to this expression is an unfolding equilibration rate, k_{unf}, of 2.84/h. Data for hydrogen exchange experiments, excepting the initial "zero point", were taken at times 1.5 h or greater. After 1.5 h, 1.4% of the protein should be native, assuming the same k_{unf} and 100% native state at $t = 0$. All later time points (3−96 h) must have $<<$1% native state. Since the kinetic data were obtained from 5 to 17 time points, depending on residue, any effect of the native state is confined to a small part of the data set. Consequently, the native state has a negligible effect on the hydrogen exchange kinetics.

Pressure and Temperature Control for Hydrogen Exchange Experiments. Temperature control was achieved with a Lauda Ultra K70DW bath circulating methanol at −15 °C. To minimize exchange during the pressurization stage, the sample was cooled to just above the freezing point of D_2O (∼+5 °C) before any pressurization was done. Renaturation, and hence quenching of hydrogen exchange, was accomplished by heating with a warm (∼20 °C) bath while pressure was released from the vessel. Both the denaturing and renaturing procedures occur quickly enough (Nash et al., 1996) that exchange during these times is negligible compared to that during the prolonged exposure to cold denaturing conditions. In particular, the establishment of cold denaturing conditions occurs in less than 30 min, well below the half-life of the most rapidly exchanging protons visible in lysozyme in D_2O (Table 1, Supporting Information).

Hydrogen Exchange Kinetics and Data Analysis. Seventeen samples were analyzed after exposure to denaturing conditions for times ranging from 0 to 96 h. After renaturation, the samples were removed from the pressure vessel, frozen for storage, and at the earliest convenient time, analyzed using proton NMR. As in previous work on RNase A (Nash et al. 1996), storage at subfreezing temperatures for times of up to 2 weeks does not affect the subsequently obtained spectra of lysozyme, within experimental error.

Spectra used for quantitative kinetic measurements were magnitude-mode proton correlation spectra (COSY), obtained on a 500 MHz Varian Unity INOVA 500NB spectrometer. All spectra consisted of 512 FIDs of 2K points each, with 8 scans per FID and a spectral width of 8000 Hz, and were taken at ambient pressure and a temperature of 20 °C. Data processing and analysis were done with Varian VNMR software, version 5.3. Processing consisted of unshifted sine bell apodization in both dimensions, along with software subtraction of the residual HDO signal. Kinetic data were obtained by volume integration of the relevant peaks in the amide fingerprint region; 52 amide peaks yielded useful integrals. These integrals (I) were referred to the average integral (I_{ref}) of cross peaks of nonexchanging ring protons in three residues (Y23, Y52, and W108). Kinetic data were obtained by fitting ln (I/I_{ref}) vs time and obtaining the slope from the least squares linear fit to the data; since the overall reaction is first order, the slope gives the observed rate constant (k_{obs}) directly. A minimum of five points was used for each fit.

RESULTS

Computation of Reference (random coil) Exchange Rates. Hydrogen exchange data for proteins are typically expressed in terms of the protection factor $P = k_{ch}/k_{obs}$ for a given amide proton, where k_{obs} is the experimentally measured exchange rate and k_{ch} the exchange rate for a proton in an ideal unstructured polypeptide under the same conditions. P values close to 1 indicate lack of appreciable structure, whereas P values in certain regions of native proteins can exceed 10^6. In partially folded states, such as molten globules (Buck et al., 1994) or the methanol-induced A state of ubiquitin (Pan & Briggs, 1992), P values are intermediate. Typical values in such states range from 1 to several hundred.

Exchange of amide hydrogens in peptides is primarily caused by acid and base, with a small contribution from water, which can act as a weak acid or base (Bai et al., 1993):

$$k_{ch} = k_a[D^+] + k_b[OD^-] + k_w \qquad (1)$$

In D_2O, the measured pH meter reading (pH*) must be corrected for the isotope effect of D_2O (pD = pH* + 0.4) (Glasoe & Long, 1959), and the calculation of [OD^-] from pD must use the pK_w of D_2O (+15.05 at ambient pressure and +25 °C) (Bai et al. 1993). The values of k_a, k_b, and k_w used in this study are based on reference values determined by measurements in D_2O (Bai et al. 1993), so isotope effects for the rate constants themselves do not need to be considered.

Values for the three rate constants are known for reference "random coil" materials, specifically unstructured oligopeptides and random-coil polypeptides, at 293 K and ambient pressure (Bai et al. 1993). To obtain a value for k_{ch} for cold denaturing conditions, the reference values were corrected for temperature and pressure by using the activation energies and the activation volumes, respectively:

$$k_i(T) = k_i(T_0)\exp\left(-\frac{E_a}{R}\left[\frac{1}{T} - \frac{1}{T_0}\right]\right) \qquad (2)$$

$$k_i(P) = k_i(P_0)\exp\left(-\frac{(P - P_0)\Delta V^{\ddagger}}{RT}\right) \qquad (3)$$

where i denotes any of the three individual reactions and E_a and $\Delta V^{\ddagger}$ are the activation energy and activation volume.

The activation volume, defined from

$$\Delta V^{\ddagger} = -RT\frac{\partial \ln k}{\partial P} \quad (4)$$

was assumed to be constant, over the pressure range of interest, to derive eq 3. This assumption has been shown to be valid over a wide pressure range for k_a and k_b in poly-D,L-lysine (Carter et al. 1978), and since the reaction mechanism for k_w is similar, this is a reasonable assumption there as well. The activation energies for k_a, k_b, and k_w are 14 kcal/mol, 3 kcal/mol, and 19 kcal/mol, respectively (Bai et al. 1993). For activation volumes, previous work on random coil poly-D,L lysine (Carter et al. 1978) has established values of 0 ± 1 and $+6 \pm 1$ cm^3/mol for k_a and k_b, respectively. For k_w, work on the small amide *N*-methylacetamide (Mabry et al. 1996) indicates a value of -9.0 ± 1.8 cm^3/mol.

The role of the water term, k_w, in amide hydrogen exchange is somewhat controversial. At ambient pressure, the k_w term is small compared to the others (Bai et al. 1993) and in many hydrogen exchange experiments is simply neglected (Perrin & Arrhenius, 1982; Molday et al., 1972). However, any water-catalyzed reaction is likely to show a large increase in rate with pressure. Since any plausible mechanism produces a separation of charges in the transition state and hence considerable solvent electrostriction, the reaction should have a large negative activation volume. Hence even a small k_w is likely to become significant at high pressure. Additionally, since the pH* used for cold denaturing lysozyme is similar to the pH_{min} for many systems (Bai et al. 1993; Robertson & Baldwin, 1991), the water exchange term is more likely to be significant, since the effect of k_w on the total rate is greatest at pH_{min}. Previous work in this laboratory (Zhang et al., 1995; Nash et al., 1996) used, as a first approximation to the activation volume for k_w, a value of -20.4 cm^3/mol, which is the reaction volume for water self-ionization (Hamann, 1963) and hence not a true activation volume. The recently measured value of -9.0 ± 1.8 cm^3/mol (Mabry et al. 1996) is considerably smaller. Nevertheless, this value is still sufficient to make the water-catalyzed component significant at the pH* and pressures actually used, when applied to the established value of k_w (Bai et al. 1993). As a result, all data in this study have been treated with the full form of the rate eq 1.

An additional correction must be applied to the deuteronium and deuteroxide ion concentrations, since the pK_w of D_2O changes with temperature (Bai et al. 1993) and pressure. Since $[D^+] >> [OD^-]$ for our samples, most of the change in ion concentrations due to changing pK_w occurs in $[OD^-]$; changes in $[D^+]$ from this cause can be neglected. After the various temperature and pressure corrections, corrections for the kinetic effects of nearest neighbor side chains, based on the recent reevaluation of these quantities by Bai et al. (1993), were applied.

A comparison of the observed exchange rates k_{obs} to the chemical exchange rate k_{ch}, defined from eq 1, requires some knowledge of the mechanism of protection. In particular, using the protection factor *P* as a measure of protein structure requires that the exchange rate be determined by k_{ch}, the chemical exchange rate, and then be modified by some kinetic effect produced by structure associated with the denatured state. If other rates, e.g., the rate of protein unfolding, determine the overall rate of hydrogen exchange, protection factors may not measure structural properties of the denatured state. It is thus necessary to verify that the kinetics occurring at extremely low temperature and high pressure permit the meaningful use of protection factors.

In most protein folding and stability studies, the overall hydrogen exchange rate is evaluated in terms of the following mechanism:

$$NH_n \underset{k_2}{\overset{k_1}{\rightleftarrows}} NH_d \xrightarrow{k_{ch}} ND \quad (5)$$

where k_1 and k_2 denote the unfolding and folding rates of the native (or otherwise highly protected) amide NH_n and the denatured state amide NH_d, and k_{ch} is the chemical exchange rate given by eq 1.

In many hydrogen exchange studies (Englander & Kallenbach, 1983), the distinction between EX1 and EX2 kinetics is made, depending on the relative magnitudes of k_2 and k_{ch}. Normally, in protein HX studies one encounters EX2 kinetics in which $k_{ch} << k_2$, and the observed rate is equal to $K_{eq}k_{ch}$ where K_{eq} is the unfolding equilibrium constant (k_1/k_2). However, these limiting cases apply (Hvidt & Nielsen, 1966; Wagner & Wüthrich, 1979) only when k_1 is small compared to k_{ch}; this is not a valid assumption under highly denaturing conditions at pHs close to the pH_{min}. Using the data in Table 1, the equilibration rate for unfolding (k_{unf}) is 2.84/h at $T = -13.2$ °C, $P = 3725$ bar. From temperature-jump kinetics, $k_{unf} = k_1 + k_2$. Since the protein is essentially completely unfolded after full equilibration, $k_1 >> k_2$ and hence $k_1 \sim k_{unf}$, or 2.84/h. By contrast the calculated random coil exchange rates, corresponding to k_{ch}, range from 0.043/h to 1.67/h depending on residue. Under these conditions, in which $k_1 >> k_2$ and $k_1 >> k_{ch}$, it can be shown that the observed hydrogen exchange rate k_{obs} approaches k_{ch}. This behavior is similar to that observed in EX2 kinetics, except that deviations in the observed exchange rate from k_{ch} result from differences in the denatured state, rather than differences in the value of the native-denatured state equilibrium. In this "pseudo-EX2" regime, therefore, deviations from k_{ch} can be meaningfully characterized by a protection factor $P = k_{ch}/k_{obs}$.

The resulting k_{ch} values were compared to the measured exchange rates (k_{obs}) to yield the protection factors (Table 1, Supporting Information). There were 52 amide protons for which kinetic data could be obtained. For each proton, statistical errors in k_{obs} based on scatter in the least-squares fits are also given; the values quoted are the standard deviation of the measured exchange rates and are below 20% for most protons. For the protection factors *P*, errors include both the errors from k_{obs} and an estimate of the error in k_{rc}; the latter is due predominantly to the fairly large uncertainties in the activation volumes. The total error is typically about 25%. Figure 2 shows the protection factors in cold-denatured lysozyme as a function of residue number and their correspondence with secondary structural elements in the native state; Figure 3 shows how the protection factors in cold-denatured lysozyme compare with those in various other well-studied denatured states—specifically, thermally denatured lysozyme at 69 °C, chemically denatured lysozyme in 8 M urea solution, and the acid denatured state of CM^{6-127} lysozyme, produced by cleaving the disulfide bond between C6 and C127 in native lysozyme (Buck et al. 1994). At

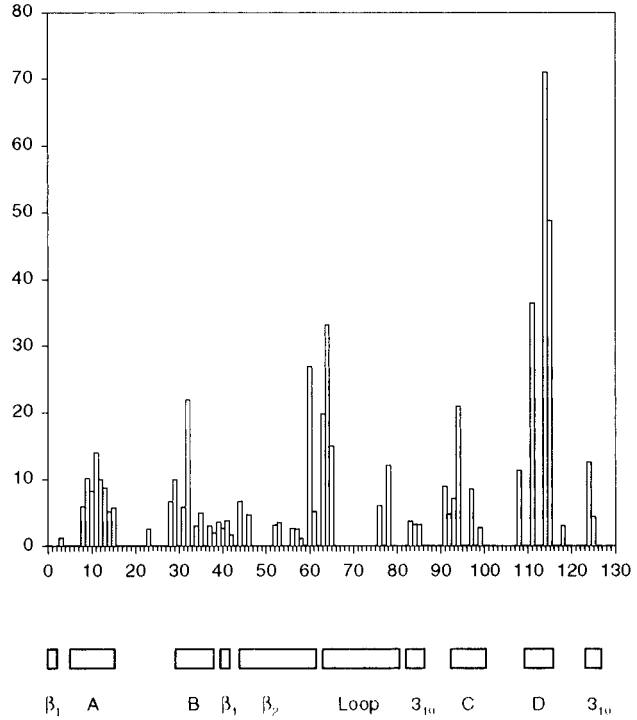

FIGURE 2: Protection factors for the pressure-assisted cold-denatured state of lysozyme. Secondary structural elements in the native state are indicated below. A−D denote the four α-helices; β_1 and β_2 denote the two and three-stranded β-sheet regions respectively.

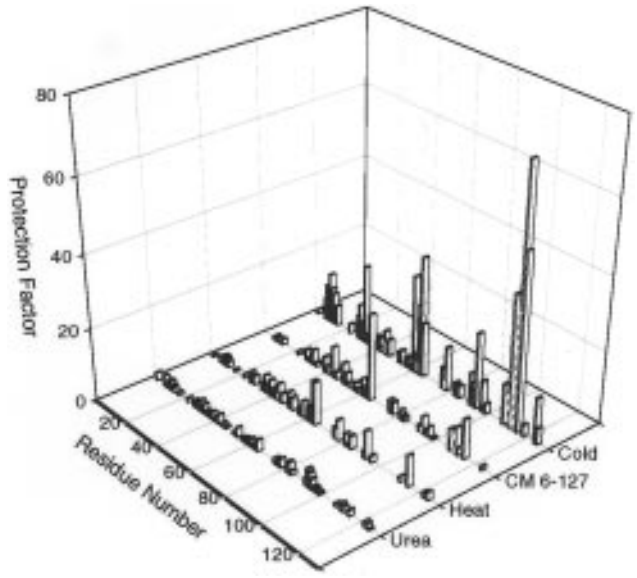

FIGURE 3: Comparison of protection factors observed in various experiments. Data for cold-denatured lysozyme were taken from this work; data for heat, urea, and acid-denatured CM^{6-127} lysozyme were taken from Buck et al., 1994.

neutral pH, CM^{6-127} lysozyme is similar in structure to the native state, though appreciably less resistant to hydrogen exchange (Eyles et al., 1994; Chung et al., 1997). However, it is less acid-stable than native lysozyme, and denatures at pH 3 or below, conditions under which native lysozyme is still highly stable.

DISCUSSION

Comparison of Pressure-Assisted Cold-Denatured State to Other Denatured States. From the hydrogen exchange rate data, it is clear that many regions of lysozyme are markedly protected from exchange, with *P* values exceeding 10, in the cold-denatured state. The range of *P* factors (Table 1, Supporting Information) runs from 1.19 for F3 to 71.0 for R114. Except for a partially folded form observed in 50% trifluoroethanol (Buck et al. 1994), cold-denatured lysozyme is the only form of denatured lysozyme that shows appreciable protection from exchange. Data for heat, urea, and acid-denatured CM^{6-127} lysozyme, analyzed using the same temperature and side chain correction methods used in this study (Buck et al. 1994), show few residues with $P > 5$ (Figure 2). It should be made clear that the pressure-assisted cold-denatured state is not a "pure" cold-denatured state, since the pressure affects the protein directly. Furthermore, the protection factors are low and incompatible with anything more than small or transiently formed regions of structure. Nevertheless, any effect that pressure and low temperature have is clearly very different from that induced by high temperature or chemical denaturants such as urea.

Lysozyme, in its native state, consists of two domains: the α-domain, which contains four α-helices, and the β-domain, which contains a 3-strand antiparallel β-sheet (Miranker et al. 1991). Various other elements of secondary structure, including two small 3^{10} helices, a small 2-stranded β-sheet, and three loops, are also present. In the cold-denatured state of lysozyme, protection of amide protons against exchange is largely confined to the α-domain; all four major α-helices in the α-domain show some protection ($P > 10$ for at least one residue) from exchange. The most notable protection, involving three residues with $P > 30$, occurs in helix D (residues 108−115). By contrast most of the β-sheet region (residues 41−60) shows no appreciable protection, with all but two residues having $P < 5$. Similarly the 3^{10} helix in the β-domain (residues 79−84) shows little protection, less than that seen in the distorted 3^{10} helix near the C-terminus in the α-domain. In most other denatured forms of lysozyme, the higher protection factors are randomly distributed throughout the sequence (Buck et al. 1994). An anomalous area of protection occurs at the end of the β-sheet and in the following loop, a region in which residues 60, 61, 63, 64, 65, 76, and 78 were observable. This region is the most highly protected area of cold-denatured lysozyme, after the D helix. It differs from the other highly protected regions in cold-denatured lysozyme, though, by not consisting of a single, well defined region of secondary structure. Figure 4 shows the tertiary structure of lysozyme, with the various strongly protected residues in the cold-denatured state labeled; the association of protected residues with the α-domain helices and portions of the loop is apparent.

Comparison of Cold-Denatured Lysozyme to Lysozyme During Refolding. A major result of lysozyme folding studies is the discovery that the α-domain folds first (Miranker et al. 1991; Radford et al. 1992). Labile amide protons in lysozyme become protected during folding through two kinetically distinct processes, a fast ($\tau < 10$ ms) and a slow ($\tau > 20$ ms) process (Radford et al. 1992). The slow phase of protection from exchange varies widely for different regions of the protein; generally, amides in the α-domain are protected from exchange much more rapidly than those in the β-domain (Radford et al. 1992). It is notable that cold-denatured lysozyme shows precisely this sort of pattern in its protection from exchange; almost all of the residues appreciably protected in the cold-denatured state are in the

FIGURE 4: Protection factors in pressure-assisted cold-denatured lysozyme. Residues observable in the cold-denatured state of lysozyme are indicated: little protection ($P < 5$), light gray circles; moderate protection ($5 < P < 10$), dark gray circles; significant protection ($P \geq 10$), black circles. This diagram was prepared with the program MolScript (Kraulis, 1991).

α-domain. Even more notable, however, are the exchange properties of observable residues at the end of the β-sheet and in the large central loop (residues 60−78). These protons are, as already seen, appreciably protected from exchange in cold-denatured lysozyme; they are also strongly protected, or relatively rapidly protected, during lysozyme folding. Specifically, residues 63, 64, and 78 show moderate to rapid ($\tau < 100$ ms) protection from exchange (Radford et al. 1992) during the slow phase of folding; kinetically, they behave more like residues in the highly protected and stable α-domain helices than the β-sheet or other β-domain regions.

More strikingly, both the α-helical and loop regions are protected in the earliest stages of folding. In a useful variant of conventional pulsed-labeling hydrogen exchange studies, Gladwin and Evans (1996) observed relatively early stages in the folding of lysozyme by confining exchange to the dead time of their instrumentation (~3.5 ms). Slowing of exchange measured during this time can be quantified by comparing the measured exchange rate to that for a random coil, as in other hydrogen exchange studies. The resulting quantity, though similar to a protection factor, is determined from a rate that changes considerably as the protein refolds; as a result, it is best referred to as a "dead time inhibition factor" (I_D) rather than a true protection factor (Gladwin & Evans, 1996). Nevertheless, I_D values provide information similar to that provided by P values in equilibrium denatured states. During the first 3.5 ms of folding, lysozyme shows moderate degrees of protection ($I_D > 5$) not only in the α-helices and the C-terminal 3^{10} helix, but also in the loop region from residues 60−65, as well as residue 78 (Gladwin & Evans, 1996). The early stages of lysozyme refolding thus show a marked resemblance to the cold-denatured state. We have thus observed a strong parallel between a stable, denatured form of lysozyme and the transient species observed during folding. Figure 5 compares the inhibition of hydrogen exchange observed during the first 3.5 ms of folding (Gladwin & Evans, 1996) to the protection factors obtained for pressure-assisted cold-denatured lysozyme.

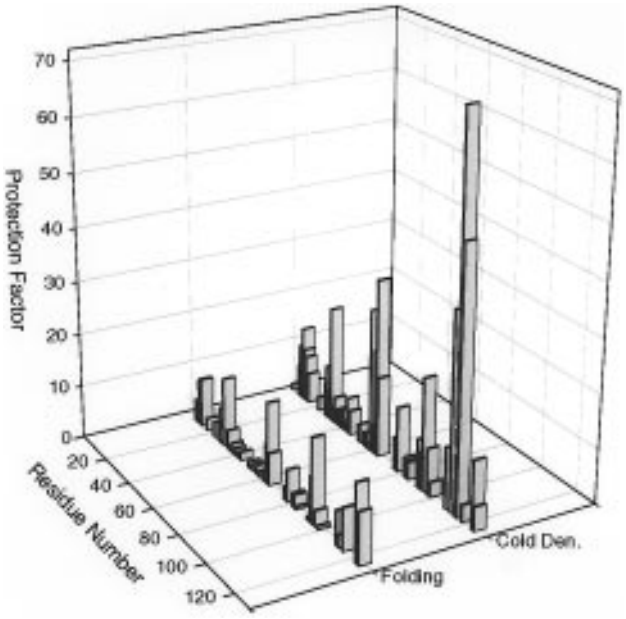

FIGURE 5: Comparison of protection factors observed in cold-denatured lysozyme to the dead time inhibition factors obtained for the first 3.5 ms of lysozyme folding (Gladwin & Evans, 1996).

Cold-Denatured Lysozyme and Cold-Denatured Ribonuclease A. The strong similarity of the cold-denatured state of lysozyme to species observed during lysozyme folding suggests the possibility of a more general phenomenon. To investigate this idea in more detail, previous data on RNase A (Nash et al. 1996) were reexamined. The original study of pressure-assisted cold-denatured RNase A was essentially identical to that of lysozyme, except in experimental conditions ($P = 3000$ bar; $T = -17$ °C) and in one key area of the data analysis: the value of the activation volume for k_w, which was assumed to be -20.4 cm^3/mol. Table 2, Supporting Information, gives values of the protection factors obtained for RNase A using the original k_{obs} values, but after recomputing k_{ch} with the activation quantities used for cold-denatured lysozyme. Errors in P were determined in the same manner as for lysozyme.

The range of protection factors observed in cold-denatured RNase A (2.8 to 78) is similar to that present in cold-denatured lysozyme. In contrast to lysozyme, however, the extent of protection in cold-denatured RNase A is less organized. Rather than having large extents of secondary structure protected, like large portions of the α-helices in lysozyme, the protection in cold-denatured RNase A occurs in small regions, particularly those near disulfide-linked cysteine residues (Nash et al. 1996). Figure 6 shows the protected residues in pressure-assisted cold-denatured RNase A on a three-dimensional representation of the native structure. The most notable such region of high protection in RNase A, three residues with $P > 10$, is centered on C84, in the central strand of the large β-sheet. Protection in this β-sheet is highly nonuniform. For example, the region of the first strand from residues 35 to 48 is essentially unprotected ($P < 5$ for all residues), in contrast to the region around C84.

Previous research on species characterized during RNase A folding (Udgaonkar & Baldwin, 1990; Houry & Scheraga, 1996) has indicated widely varying degrees of structure among them. Additionally, unfolded RNase A is heterogeneous because of isomerization about X-Pro bonds; this

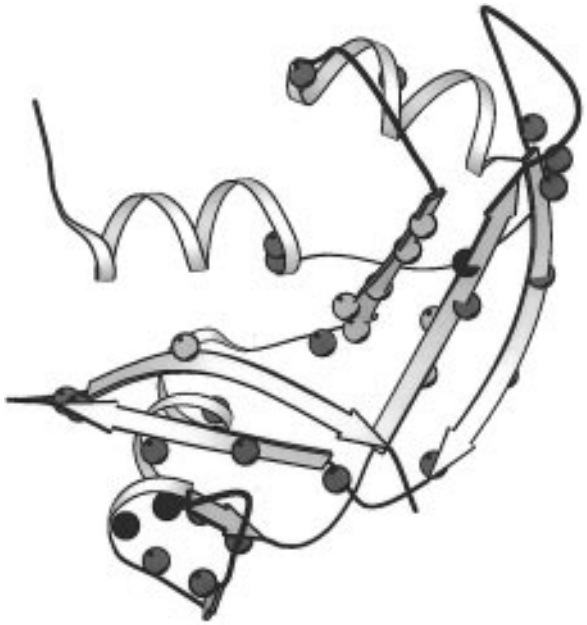

FIGURE 6: Protection factors for the pressure-assisted cold-denatured state of RNase A. For ease of comparison, the color scheme is the same as that for Figure 7, i.e., residues with $1.5 < P < 5$ are in light gray; those with $5 < P < 50$, dark gray; and those with $P > 50$, black. This diagram was prepared with the program MolScript (Kraulis, 1991).

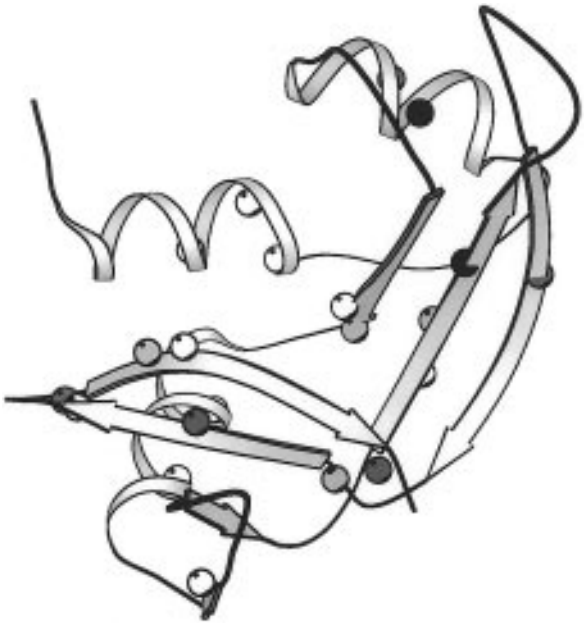

FIGURE 7: Protection factors for I_Φ, the folding intermediate for RNase A refolding from U_{vf} (Houry & Scheraga, 1996). The color scheme follows the four classes of protection distinguished by Houry and Scheraga: Unprotected residues ($P < 1.5$) are colored white; weakly protected residues ($1.5 < P < 5$), light gray; moderately protected residues ($5 < P < 50$), dark gray; strongly protected residues ($P > 50$), black. This diagram was prepared with the program MolScript (Kraulis, 1991).

heterogeneity strongly affects the types of species that are observed during folding. Two folding pathways of RNase A have been studied in detail by hydrogen exchange methods. When RNase A is allowed to unfold and equilibrate, the dominant unfolded form is U_S^{II}, in which isomerization of X-Pro bonds has occurred. The folding process from this unfolded species has been elucidated in detail (Udgaonkar & Baldwin, 1990) using conventional pulsed-labeling hydrogen exchange techniques. On renaturing from U_S^{II}, RNase forms a highly structured species, I_1, by 0.1 s. Folding continues to the highly nativelike species I_N, which differs from I_1 by proline isomerization and has catalytic activity (Udgaonkar & Baldwin, 1990):

$$U_S^{II} \rightarrow I_1 \rightarrow I_N \rightarrow N$$

By varying the pH of the labeling pulses, Udgaonkar and Baldwin were able to determine rough values for the protection factors in the intermediates. In I_1, the β-sheet is extensive and highly protected. I_1 is probably heterogeneous, since protection increases with refolding time. After 0.1 s, P values of roughly 100 are typical in I_1, but by 0.4 s, I_1 has 13 residues with $P \geq 1000$.

U_S^{II} forms when denatured RNase A has sufficient time to undergo isomerization about proline residues. When folding is initiated after only 1 s of unfolding, there is insufficient time for cis−trans isomerization around proline residues, and the predominant unfolded form is U_{vf}, which contains no wrongly oriented X-Pro bonds. U_{vf} refolds much more rapidly than U_S^{II}. By using a similar pulsed-labeling hydrogen exchange technique, Houry and Scheraga characterized the species produced on folding from U_{vf} (Houry & Scheraga, 1996). In folding from U_{vf}, a largely unfolded species I_U, followed by a molten-globule-like species I_Φ, can be characterized:

$$U_{vf} \rightarrow I_U \rightarrow I_\Phi \rightarrow N$$

Under near-native conditions (0.7 M Gdn-HCl, pH 9.0), the formation of these species is much more rapid than the formation of I_1 from U_S^{II}; they form in the dead time ($t \sim 2$ ms) of conventional stopped-flow apparatus (Houry & Scheraga, 1996). A detailed kinetic study at variable denaturant concentration and pH, with short folding and labeling stages, is needed to fully characterize the intermediate species; Houry and Scheraga used a 6 ms refolding stage, in contrast to >100 ms for measurements on U_S^{II}.

On folding from the U_{vf} state, no species are observed with protection factors comparable to those in I_1. The intermediate I_U is essentially unprotected and I_Φ shows protection factors similar to those in equilibrium molten globules, i.e., P values from 1 to ~100. Figure 7 shows the protected residues in I_Φ on a three-dimensional representation of the native structure of RNase A.

The cold-denatured state of RNase A bears little resemblance to I_1; the protection factors and degree of secondary structure in this species are much too large. Specifically, the β-sheet in I_1 is extensive, whereas large stretches of the β-sheet region in the cold-denatured state of RNase A are essentially unstructured. I_Φ, however, bears considerable resemblance to the cold-denatured state of RNase A. Despite having a limited number of NMR-visible resonances to work with, Houry and Scheraga found seven residues in I_Φ that have $P > 5$, two of which, M29 and C84, have $P > 100$. In cold-denatured RNase A, the region around C84 shows moderate to strong protection, with C84 itself having the second largest P value in cold-denatured RNase A ($P = 58$).

Unfortunately, M29 was not observable in the cold-denatured state; its peak was too weak for integration. M29 is, however, in a helix (residues 24−35) that has two other observable residues with moderate ($P \sim 10$) protection in the cold-denatured state. Since the number of probes in Houry and Scheraga's study was limited, a more detailed comparison of I_Φ to the cold-denatured state is difficult. The extent of structure in the cold-denatured state appears to be larger than that in I_Φ; in particular, considerably more residues with $P > 5$ are noted (25 in the cold-denatured state vs 7 in I_Φ), and specific structural elements like helix 3 (residues 50−60) show considerably more protection.

General Conclusions. Protein folding is thought to proceed initially by a period of rapid hydrophobic collapse, during which secondary structure begins to form and modest amounts of protection from exchange ($P \sim 10-100$) may occur. Collapse can be very rapid, with considerable structural reorganization occurring within the dead time of conventional pulse labeling hydrogen exchange techniques. For example, measurements of Trp fluorescence show that significant structural changes in apomyoglobin occur less than 20 μs after folding begins (Ballew et al. 1996). At somewhat longer time scales ($t \sim 10$ ms) molten-globule like intermediates have been characterized for apomyoglobin and cytochrome *c* (Ptitsyn, 1995).

In lysozyme, the earliest stages of folding are characterized by protection of many of the α-domain residues and part of the loop (Gladwin & Evans, 1996), which shows the structure in the α-domain begins to form extremely quickly. One possible explanation is that lysozyme in both the cold-denatured state and in the early stages of refolding is a relatively stable molten globule, characterized by formation of portions of secondary structure and little or no persistent tertiary structure. Many molten globules are more stable versions of the hydrophobically collapsed state proposed as a very early step in protein folding. Normally, lysozyme does not form a molten globule readily, particularly when compared to proteins like α-lactalbumin. High pressure, however, favors reactions with less positive reaction volumes; the relatively compact molten globule state may thus be more readily observable at high pressure than at ambient pressure, since formation of the molten globule state involves a smaller volume increase than complete unfolding does.

In RNase A, existing studies are less clear on the relation between folding intermediates and the cold-denatured state. I_1 does not resemble the cold-denatured state much at all. However, I_1 is unlikely to be the first species with considerable structure occurring when RNase A folds; though I_1 is the first well-characterized intermediate for RNase A refolding from U_S^{II}, it is a relatively slowly appearing species, so it is unlikely to be a good indicator of the early folding properties of RNase A. The earliest well-defined structure should form much earlier, be less extensive, and be characterized by much weaker protection from hydrogen exchange. I_Φ forms much more rapidly than I_1, albeit from a different isomer of unfolded RNase A, and is characterized by weaker protection from exchange, as would be expected for an earlier folding species. It is thus significant that the cold-denatured state of RNase A qualitatively resembles I_Φ, in the extent and location of moderate protection factors. Further work on the folding of RNase A from U_S^{II} should reveal a partially folded state, possibly not a true intermediate, with patchy distributions of high protection including a region near C84, which is highly protected in I_1, I_Φ, and the cold-denatured state of RNase A.

By investigating a novel method of denaturation, the existence of partially folded states of two well-studied proteins was verified, and the degree of structure present in them characterized. The extent of structure in pressure-assisted cold-denatured lysozyme and RNase A exceeds that present in most other denatured forms of these proteins, particularly heat and chemical denaturation, in which structure is extremely tenuous and unstable if it exists at all. More interestingly, though, both the extent and the stability of residual structure in cold-denatured lysozyme and RNase A are similar to those found in early folding ($t < 10$ ms) species of these proteins. Lysozyme and RNase A are notable for having some interesting complications in their folding kinetics, induced by multiple domain behavior and proline isomerization, respectively. Proteins that show little such complication, e.g., ubiquitin, would be a good test of the validity of the hypothesis we have outlined; the exchange kinetics of cold-denatured ubiquitin are currently being studied in our laboratory. It is our intention to continue various studies of pressure- and pressure-assisted cold denaturation on other proteins, in order to obtain novel information about their folding intermediates, or to simply indicate key stable structures favored preferentially in the folding process.

ACKNOWLEDGMENT

NMR data was collected on a spectrometer in the University of Illinois School of Chemical Sciences Varian/Oxford Instrument Center for Excellence in NMR Laboratory. We acknowledge NIH grant 1-S10-RR-10444-01, the Keck Foundation, and the Beckman Institute for their contributions to this laboratory.

SUPPORTING INFORMATION AVAILABLE

Tables of measured hydrogen exchange rates and protection factors, including error estimates, for cold-denatured lysozyme (Table 1) and for cold-denatured ribonuclease A (Table 2) (5 pages). Ordering information is given on any current masthead page.

REFERENCES

Bai, Y., Milne, J. S., Mayne, L., & Englander, S. W. (1993) *Proteins: Struct. Funct. Gene. 17*, 75−86.

Ballew, R. M., Sabelko, J., & Gruebele, M. (1996) *Proc. Natl. Acad. Sci. U.S.A. 93*, 5759−5764.

Buck, M., Radford, S. E., & Dobson, C. M. (1994) *J. Mol. Biol. 237*, 247−254.

Carter, J. V., Knox, D. G., & Rosenberg, A. (1978) *J. Biol. Chem. 253*, 1947−1953.

Chung, E. W., Nettleton, E. J., Morgan, C. J., Gross, M., Miranker, A., Radford, S. E., Dobson, C. M., & Robinson, C. V. (1997) *Protein Sci. 6*, 1316−1324.

Creighton, T. E. (1990) *Protein Folding*. W. H. Freeman & Co., New York.

Dill, K. A., & Shortle, D. R. (1991) *Annu. Rev. Biochem. 60*, 795−825.

Dyson, H. J., & Wright, P. E. (1996) *Annu. Rev. Phys. Chem. 47*, 369−395.

Englander, S. W., & Kallenbach, N. L. (1983) *Quart. Rev. Biophys. 16*, 521−655.

Eyles, S. J., Radford, S. E., Robinson, C. V., & Dobson, C. M. (1994) *Biochemistry 33*, 13038−13048.

Fink, A. L. (1995) *Annu. Rev. Biophys. Biomol. Struct. 24*, 495−522.
Gladwin, S. T., & Evans, P. A. (1996) *Folding and Design 1*, 407−417.
Glasoe, P. K., & Long, F. A. (1959) *J. Phys. Chem. 64*, 188−193.
Hamann, S. D. (1963) *J. Phys. Chem. 67*, 2233−2235.
Houry, W. A., & Scheraga, H. A. (1996) *Biochemistry 35*, 11734−11746.
Hvidt, A., & Nielsen, S. O. (1966) *Adv. Protein Chem. 21*, 287−386.
Jonas, J., & Jonas, A. (1994) *Annu. Rev. Biophys. Biomol. Struct. 23*, 287−318.
Jonas, J., Koziol, P., Peng, X., Reiner, C., & Campbell, D. M. (1993) *J. Magn. Reson. B. 102*, 299−303.
Kim, P. S., & Baldwin, R. L. (1990) *Annu. Rev. Biochem. 59*, 631−660.
Kitamura, Y., & Itoh, T. (1987) *J. Solut. Chem. 16*, 715−725.
Kraulis, P. J. (1991) *J. Appl. Crystallogr. 24*, 946−950.
Mabry, S. A., Lee, B., Zheng, T., & Jonas, J. (1996) *J. Am. Chem. Soc. 118*, 8887−8890.
Molday, R. S., Englander, S. W., & Kallen, R. G. (1972) *Biochemistry 11*, 150−158.
Miranker, A., Radford, S. E., Karplus, M., & Dobson, C. M. (1991) *Nature 349*, 633−636.
Nash, D., Lee, B., & Jonas, J. (1996) *Biochimica et Biophysica Acta 1297*, 40−48.
Pan, Y., & Briggs, M. S. (1992) *Biochemistry 31*, 11405−11412.
Perrin, C. L., & Arrhenius, G. M. L. (1982) *J. Am. Chem. Soc. 104*, 6693−6696.
Privalov, P. L. (1990) *CRC Crit. Rev. Biochem. Mol. Biol. 25*, 181−305.
Ptitsyn, O. B. (1995) *Curr. Opin. Struct. Biol. 5*, 74−78.
Radford, S. E., Dobson, C. M., & Evans, P. A. (1992) *Nature 358*, 302−307.
Redfield, C., & Dobson, C. M. (1988) *Biochemistry 27*, 122−136.
Robertson, A. D., & Baldwin, R. L. (1991) *Biochemistry 30*, 9907−9914.
Samarasinghe, S. D., Campbell, D. M., Jonas, A., & Jonas, J. (1992) *Biochemistry 31*, 7773−7778.
Udgaonkar, J. B., & Baldwin, R. L. (1990) *Proc. Natl. Acad. Sci. U.S.A. 87*, 8197−8201.
Wagner, G., & Wüthrich, K. (1979) *J. Mol. Biol. 134*, 75−94.
Zhang, J., Peng, X., Jonas, A., & Jonas, J. (1995) *Biochemistry 34*, 8631−8641.

BI970881V